

# Nopol synthesis over Sn-MCM-41 and Sn-kenyaite catalysts

Aída Luz Villa de P, Edwin Alarcón, Consuelo Montes de C\*

*Chemical Engineering Department, Universidad de Antioquia, Calle 67 No. 53-108, Medellín, Colombia*

Available online 19 August 2005

## Abstract

Several methods were used to prepare Sn loaded kenyaite and MCM-41 silicates: ion exchange, incipient wetness impregnation and chemical vapor deposition. Catalysts were evaluated for nopol synthesis by the Prins condensation of  $\beta$ -pinene and paraformaldehyde. The resulting catalysts were characterized by elemental analysis, TGA, XRD, FTIR, BET surface area and UV–vis. Kenyaite samples modified with Sn by ion exchange were more resistant to leaching than those modified by chemical vapor deposition (CVD), while Sn-MCM-41 samples prepared by CVD were more active, selective to nopol and resistant to leaching than Sn-MCM-41 prepared by impregnation. In general, Sn-MCM-41 catalysts even at low Sn loadings exhibited higher nopol yields than Sn-kenyaite.

© 2005 Elsevier B.V. All rights reserved.

**Keywords:** Nopol;  $\beta$ -Pinene; Prins reaction; Kenyaite; MCM-41; CVD; Ion exchange; Sn

## 1. Introduction

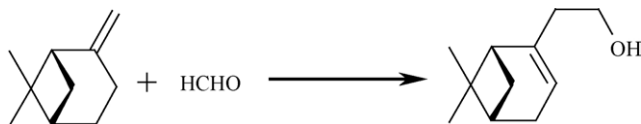
Nowadays, clean technologies are of prime importance. Catalytic processes that replace traditional methodologies are being highly investigated. Catalytic production of nopol might be a promising process. Nopol is an optically active bicyclic primary alcohol, useful in the agrochemical industry for the synthesis of pesticides, soap fragrances and household products [1]. This alcohol has been traditionally produced by condensation of  $\beta$ -pinene and paraformaldehyde in a homogeneous catalytic system (Scheme 1). Three general methods have been used to obtain nopol [2]. (1) Saponification of nopyl acetate produced from  $\beta$ -pinene and paraformaldehyde in acetic acid solution at 120 °C. (2) Heating a mixture of  $\beta$ -pinene and paraformaldehyde in the presence of a small quantity of a homogeneous catalyst such as zinc chloride. In both methods, monocyclic isomers and other side products are formed. (3) Autoclaving paraformaldehyde and  $\beta$ -pinene at 150–230 °C for several hours yields quantitative amounts of pure nopol.

Recently, nopol yields higher than 90% were obtained using a truly heterogeneous Sn-MCM-41 catalyst containing

0.51 mmol SnCl<sub>4</sub>/g of catalyst in which Sn was grafted by chemical vapor deposition (CVD) of SnCl<sub>4</sub> on MCM-41 [3]. MCM-41 is a mesoporous silicate consisting of a highly ordered hexagonal array of unidimensional pores with a very narrow pore size distribution, and a highly specific surface area of up to 1000 m<sup>2</sup>/g. The advantages of using ordered mesoporous solids for nopol production from  $\beta$ -pinene are the relatively large pores which facilitate mass transfer of these bulky compounds and the very high surface area, which allows a high concentration of active sites per mass of material [4]. More recently, a mesoporous iron phosphate has been reported as an active and recyclable heterogeneous catalyst for the selective synthesis of nopol at 80 °C with acetonitrile as solvent [5]. Notwithstanding, the amount of Fe for obtaining 100% nopol yield (1321  $\mu$ mol Fe/mmol  $\beta$ -pinene) is quite high compared to the amount of tin required in Sn-MCM-41 for nopol yields up to 98% (24  $\mu$ mol Sn/mmol  $\beta$ -pinene). On the other hand, interest in layered silicates such as kanemite, magadiite and kenyaite, has increased recently since they possess ion-exchange, adsorption, intercalation and swelling properties. These materials can be used not only as ion exchangers and adsorbents, but also, they can be transformed into new ordered mesoporous materials, which can be useful for processing bulky molecules. The basic structures of layered silicates are

\* Corresponding author.

*E-mail address:* [cmontes@quimbaya.udea.edu.co](mailto:cmontes@quimbaya.udea.edu.co) (C. Montes de C).



Scheme 1. Prins condensation of  $\beta$ -pinene and formaldehyde to nopol.

composed of duplicated  $\text{SiO}_4$  tetrahedral sheets and are similar to clay minerals with no aluminium [6–8]. Kenyaite is a well crystallized layered silicate with large basal spacings which can be pillared to obtain high surface area derivatives [9]. In this contribution, we evaluated the synthesis of nopol from  $\beta$ -pinene and paraformaldehyde over Sn modified MCM-41 and kenyaite.

## 2. Experimental

Myristyltrimethylammonium bromide (MTABr or cetrimide, 99 wt%), tin chloride ( $\text{SnCl}_4$ , 99.995 wt%),  $\beta$ -pinene (99 wt%) and paraformaldehyde (95 wt%) were purchased from Aldrich. Toluene (99.5 wt%) and acetone (99.5 wt%) were products from Mallinckrodt, tetraethoxysilane (TEOS, 98 wt%) from Acros Organics, aqueous ammonia ( $\text{NH}_4\text{OH}$ , 28–30 wt%) from EM Science and sodium hydroxide from Carlo Erba.

### 2.1. Catalyst preparation

#### 2.1.1. Na-kenyaite (Na-Ken)

The procedure reported by Kwon et al. was followed to prepare Na-Ken [8]. A gel having a composition of  $80\text{SiO}_2:2\text{NaOH}:\text{Na}_2\text{CO}_3:800\text{H}_2\text{O}$  was heated at  $180^\circ\text{C}$  under autogeneous pressure during 72 h. The solid was washed with deionized water and dried at  $65^\circ\text{C}$ .

#### 2.1.2. Tin kenyaite prepared by ion exchange (Sn-Ken-A and Sn-Ken-B)

$\text{SnCl}_4$  (400–500  $\mu\text{l}$ ) was added to a suspension of Na-Ken (1 g) into 100 ml of deionized water and the mixture stirred at room temperature for 24 h. Then, the solid was recovered and exhaustively washed with deionized water until negative chloride test. Finally, the solid was dried at  $100^\circ\text{C}$  overnight.

#### 2.1.3. Tin kenyaite prepared by CVD (Sn-Ken-C)

Na-Ken (0.2 g) was exposed to the vapor produced by 0.2 ml of  $\text{SnCl}_4$  at  $100^\circ\text{C}$  in a Teflon-lined SS autoclave under autogeneous pressure. After about 8 h, the sample was removed from the autoclave and washed with deionized water until negative chloride test. Finally, the solid was dried at  $100^\circ\text{C}$  overnight.

#### 2.1.4. Sn loaded MCM-41

The method reported by Grün et al. was followed to prepare MCM-41 [10]. Sn was incorporated on MCM-41 by

CVD (Sn-MCM-41-D), as we previously reported [3]. The amount of  $\text{SnCl}_4$  varied between 19 and 1200  $\mu\text{l/g}$  support. Sn impregnated MCM-41 (Sn-MCM-41-I) was prepared by stirring 1.0 g of MCM-41 in a 0.05 M aqueous solution of  $\text{SnCl}_4$ . After 24 h, the recovered solid was washed with deionized water and calcined at  $550^\circ\text{C}$ .

### 2.2. Catalyst characterization

Elemental analysis was carried out by atomic absorption in a Philips PU9200 instrument. Thermogravimetric analyses of selected samples were performed in a TGA 2950 from TA Instruments. XRD was carried out in an AXS Bruker diffractometer with  $\text{Cu K}\alpha$  radiation. IR spectra were recorded using a Mattson FTIR 5000 spectrometer by the KBr technique. Single point BET surface areas were determined by  $\text{N}_2$  adsorption at  $-196^\circ\text{C}$  (77 K) using an ASAP 2010 instrument. The UV–vis diffuse reflectance spectra of selected samples were obtained using a Perkin-Elmer Lambda 9 spectrometer.

### 2.3. Catalytic tests

Catalytic experiments were performed in a 3 ml reactor immersed in a temperature controlled oil bath. In a typical reaction,  $\beta$ -pinene (0.25 or 0.5 mmol), paraformaldehyde (0.5 or 1 mmol), toluene (0.5 or 1 ml) and catalyst (25 or 50 mg) were stirred at  $90^\circ\text{C}$  for several hours (1–6.5 h). After reaction, catalyst was recovered by filtration, and then exhaustively washed with acetone at  $50^\circ\text{C}$  and dried at  $100^\circ\text{C}$  before being reused. Reaction products were analyzed in a VARIAN STAR 3400 Gas Chromatograph using a FID detector and a DB-1 capillary column (50 m  $\times$  320  $\mu\text{m}$   $\times$  1.20  $\mu\text{m}$ ). The initial and final oven temperatures were 110 and  $195^\circ\text{C}$ , and detector temperatures 200 and  $280^\circ\text{C}$ , respectively. The carrier gas through the column was flowing helium (1.63 ml/min).

## 3. Results and discussion

### 3.1. Catalyst characterization

#### 3.1.1. Elemental analysis and surface area

Table 1 shows elemental tin and sodium composition for kenyaite supported catalysts. The efficiency of Sn incorporation was calculated as the molar ratio between the initial amount of  $\text{SnCl}_4$  in solution and Sn loading of the obtained material. As can be observed in Table 1, tin loading of ion exchanged kenyaite materials (Sn-Ken-A, Sn-Ken-B) is higher than that of Sn-Ken synthesized by CVD. The specific surface area of Sn loaded kenyaite materials increased and sodium decreased compared to Na-Ken. As reported by Eugster [9] magadiite and kenyaite in dilute acid solutions are converted to a crystalline hydrate of silica  $6\text{SiO}_2\cdot\text{H}_2\text{O}$ . Furthermore, sodium content of synthetic

Table 1  
Synthesis conditions and characteristics of Sn-kenyaite catalysts

Catalyst	Synthesis method	mmol Sn/g kenyaite <sup>a</sup>	Area (m <sup>2</sup> /g)	mmol/g kenyaite (wt%) <sup>b</sup>		Sn deposited (%)
				Sn	Na	
Na-Ken			102	0	0.66 (1.5)	
Sn-Ken-A	I.E.	3.41	168	1.06 (11.2)	0.02 (0.05)	31.1
Sn-Ken-B	I.E.	4.27	191	4.05 (32.5)	0.009 (0.02)	94.8
Sn-Ken-BR <sub>3</sub>			62	4.05 (32.5)	n.d.	
Sn-Ken-C	CVD	8.53	139	0.41 (4.64)	0.46 (1.04)	4.8
Sn-Ken-CR <sub>2</sub>			106	0.29 (3.37)	n.d.	

I.E.: ion exchange. R<sub>x</sub> indicates that the catalyst has been reused *x* times.

<sup>a</sup> Amount used for catalyst preparation.

<sup>b</sup> By atomic absorption, n.d. not determined.

Na-Magadiite depends on the extent of water washing [11]. Leaching of interlayer Na<sup>+</sup> cations in Na-Magadiite via hydrolysis was observed by Dailey and Pinnavia [11] by repeated washing with water. Therefore, the observed variations in Na content for different tin modified kenyaite samples are attributed to both differences in the extent of water washing of Na-Ken precursor and to Na<sup>+</sup> hydrolysis during the ionic exchange process, since SnCl<sub>4</sub> aqueous solution is slightly acidic. TGA curves in Fig. 1a show an initial weight loss of 3.4% as water below 200 °C. An additional 1.2% by weight is lost between 200 and 800 °C. The weight loss above 200 °C is assigned to dehydroxylation of SiOH groups. Adsorbed water in Sn-Ken-B is lost at higher temperatures. About 5.5% of the total weight is lost up to 500 °C and 6% between 500 and 800 °C. Therefore, Sn-Ken-B appears to contain more SiOH groups than Na-Ken suggesting that Na<sup>+</sup> cations were probably exchanged by H<sup>+</sup> instead of Sn<sup>4+</sup>. Further evidences are consistent with our conclusion. From chemical analyses the amount of Sn loaded in Sn-Ken-B (4.05 mmol/g) is much higher than the initial amount of exchangeable Na<sup>+</sup> ions (0.66 mmol/g). Besides, XRD diffraction data (vide infra) indicates decrease in the interlaminar distance of Sn-Ken-B as compared to Na-Ken. Earlier attempts to intercalate robust cations into Na<sup>+</sup>-magadiite by ion exchange also failed [11].

Sn-Ken-C samples showed the lowest surface area. Besides, sodium content is lower than in the parent Na-Ken likely due to the extent of washing. However, Na-Ken-C contains more sodium than Na-Ken-B indicating that Sn introduced by CVD reacted with surface sylanols and the extent of Na<sup>+</sup> hydrolysis was limited as compared to ion exchange method. After reaction, both surface area and Sn content decreases in Sn-Ken-CR<sub>2</sub>. No change in Sn content is observed in Sn-Ken-BR<sub>3</sub> after reaction even though its surface area decreased. Used catalyst samples have lower surface area than fresh materials more likely due to the presence of residual reactants and/or products.

Sn deposition efficiencies for Sn-MCM-41 prepared by CVD varied between 8.0 and 35.4% (see Table 2). The amount of Sn in solid samples increased as the amount of SnCl<sub>4</sub> increased and then leveled at around 5.0 mmol/g catalyst. Higher amounts of precursor did not further increase Sn loading of MCM-41. The specific surface area of Sn-MCM-41 decreased by increasing Sn content in the gel, for example, MCM-41 (1202 m<sup>2</sup>/g) > Sn-MCM41-D1 (1188 m<sup>2</sup>/g) > Sn-MCM-41-D4 (1072 m<sup>2</sup>/g) > Sn-MCM-41-D6 (1056 m<sup>2</sup>/g).

### 3.1.2. XRD analysis

The XRD pattern of kenyaite shows high intensity peaks in 3°–35° (2θ) region. In this work, we were interested on

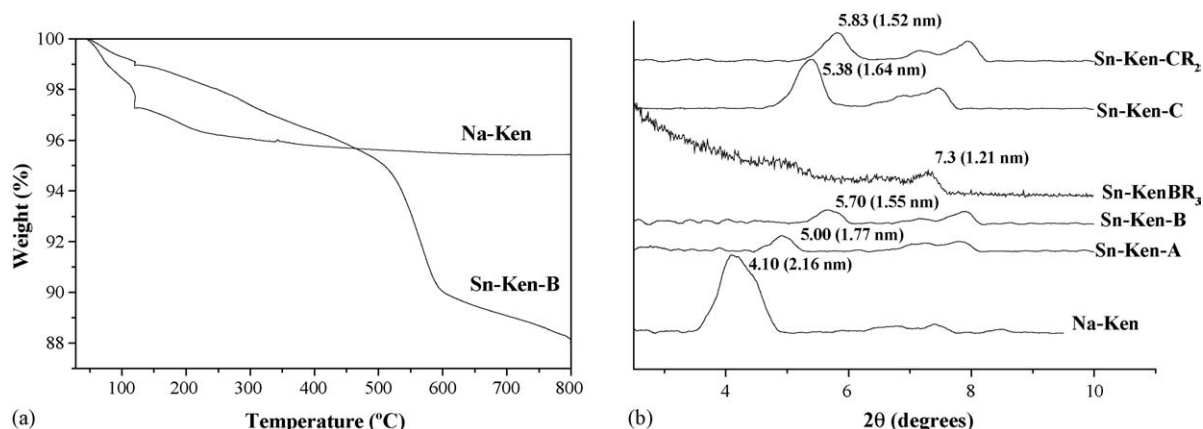


Fig. 1. (a) TGA of Na-Ken and Sn-Ken-B. (b) XRD of Sn-kenyaite materials.

Table 2  
Sn content of Sn-MCM-41 catalysts

Catalyst	Deposition time (h)	mmol SnCl <sub>4</sub> /g MCM-41 <sup>a</sup>	mmol Sn/g catalyst (wt%) <sup>b</sup>	Sn deposited (%)
Sn-MCM-41-D1	8	0.16	0.03 (0.4)	18.9
Sn-MCM-41-D2	8	0.32	0.07 (0.9)	21.9
Sn-MCM-41-D3	8	0.64	0.09 (1.1)	14.1
Sn-MCM-41-D4	8	1.27	0.45 (5.4)	35.4
Sn-MCM-41-D5	8	2.54	0.50 (5.9)	19.7
Sn-MCM-41-D6	8	5.09	0.82 (9.8)	16.1
Sn-MCM-41-D7	8	10.18	0.82 (9.8)	8.0
Sn-MCM-41-I	24	5.00	2.98 (35.5)	59.6 <sup>c</sup>

<sup>a</sup> Amount used during catalyst preparation.

<sup>b</sup> By atomic absorption.

<sup>c</sup> Sn impregnated.

monitoring changes in basal spacing given by (0 0 1) reflections at  $2\theta$  values around  $4^\circ$  [12]. As can be observed in Fig. 1b, the characteristic peak of kenyaite at  $2\theta = 4.1^\circ$ , is shifted to  $5.00^\circ$ ,  $5.38^\circ$  and  $5.70^\circ$  in Sn-Ken-A, Sn-Ken-C, Sn-Ken-B, respectively. So, the interlaminar distance decreased from 2.16 to 1.77 nm, 1.64 and 1.55 nm, respectively. The interlaminar distance also decreased in used catalysts. This decrease was more significant in Sn-Ken-BR<sub>3</sub> than in Sn-Ken-CR<sub>2</sub>. The decrease in basal spacing may be ascribed to a loss of interlayer H<sub>2</sub>O upon replacement of Na<sup>+</sup> by H<sup>+</sup>. XRD patterns for all synthesized MCM-41 materials (see Fig. 2) exhibit a strong (1 0 0) reflection peak with two small peaks, characteristic of MCM-41 type materials [10,13]. In most samples, the higher

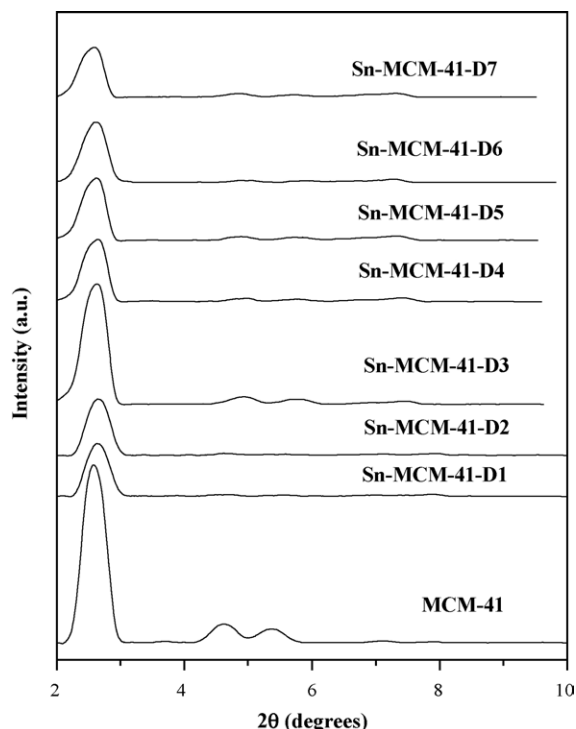


Fig. 2. XRD of Sn-MCM-41 catalysts.

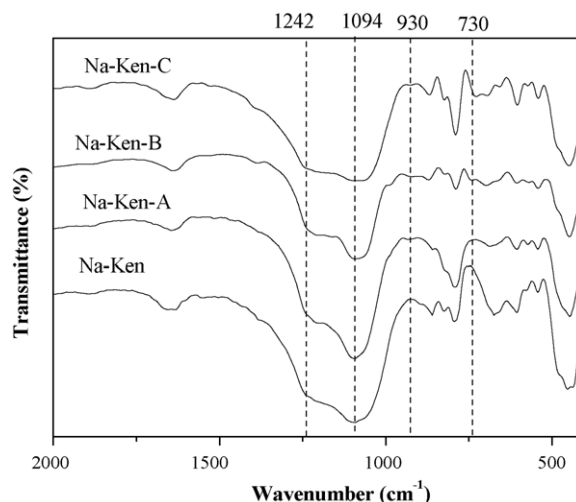


Fig. 3. IR of Sn-kenyaite materials.

the Sn loading the lower the intensity of the peak at about  $2\theta = 3.0^\circ$ . No peaks were observed in the XRD patterns of Sn-MCM-41-I (not shown).

### 3.1.3. IR spectra

Fig. 3 shows the infrared spectra of Sn-kenyaite materials. The vibration spectra of kenyaite can be split

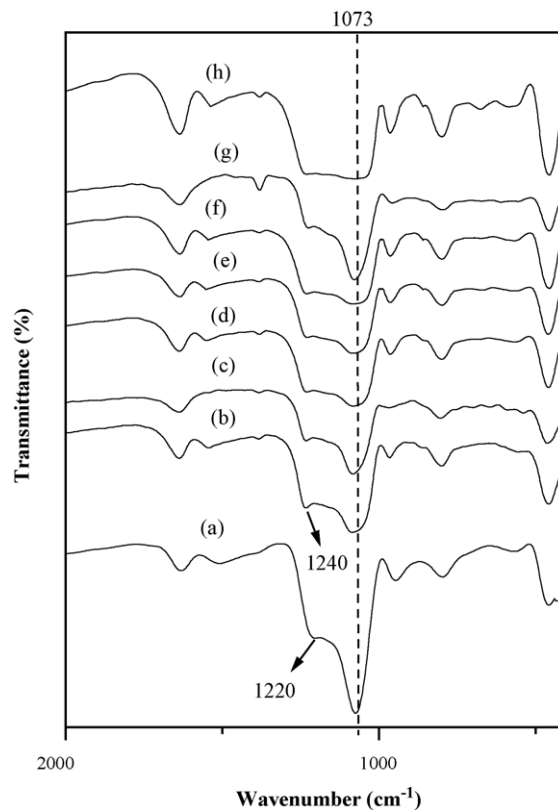


Fig. 4. IR of selected MCM-41 supported catalysts. MCM-41 (a), Sn-MCM-41-D1 (b), Sn-MCM-41-D2 (c), Sn-MCM-41-D3 (d), Sn-MCM-41-D4 (e), Sn-MCM-41-D5 (f), Sn-MCM-41-D6 (g), Sn-MCM-41-D7 (h).

in two regions [14]. The stretching and bending vibrations of water molecules appear between  $4000$  and  $1600\text{ cm}^{-1}$ . At frequencies below  $1300\text{ cm}^{-1}$  vibrations are ascribed to silicate layers and charge balancing cations [14]. All materials have the characteristic bands of kenyaite [14], including a band around  $1242\text{ cm}^{-1}$  typical of materials containing five membered rings in their structure. The  $930\text{ cm}^{-1}$  IR absorption band has been ascribed to vibration of strained (defect) T–O–Si linkages where the T atoms are not tetrahedrally coordinated [15]. Moreover, Sn-Ken-B and Sn-Ken-C catalysts show a band around  $730\text{ cm}^{-1}$  assigned to different Sn oxygen-bridged species [16].

Fig. 4 shows the infrared spectra of MCM-41 and Sn-MCM-41-D samples. Both spectra are similar, except for the shift from  $1220$  to  $1240\text{ cm}^{-1}$  observed in the Sn loaded materials. A shift to lower wavenumbers of the T–O–T lattice vibration around  $1073\text{ cm}^{-1}$  was not observed after treatment with the Sn precursor, suggesting that Sn does not substitute Si in the lattice of MCM-41 materials [17].

### 3.1.4. UV-vis spectra

UV-vis diffuse reflectance spectra of tin kenyaite and MCM-41 supported materials are shown in Figs. 5 and 6, respectively. For Sn-Ken materials band intensities increase with Sn content. An absorption band observed at  $214\text{ nm}$  in ion exchanged Sn-Ken materials may be assigned to  $\text{Sn}^{4+}$  in tetrahedral coordination [18]. However, this band is broad and could overlap with a band at  $230\text{ nm}$ . In materials prepared by CVD, the absorption band is observed at  $236\text{ nm}$  in kenyaite and at  $242\text{ nm}$  in Sn-MCM-41 materials. These bands are close to  $230\text{ nm}$  assigned to hexacoordinated Sn

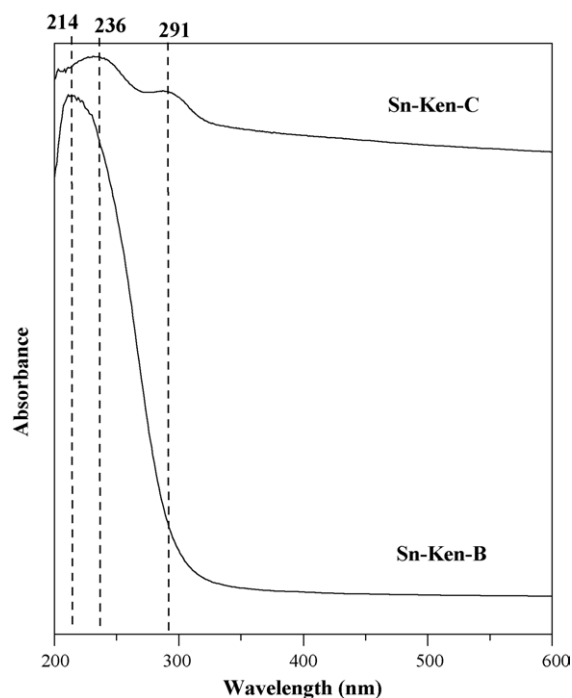


Fig. 5. Diffuse reflectance UV-vis spectra of Sn-Ken-B and Sn-Ken-C catalysts.

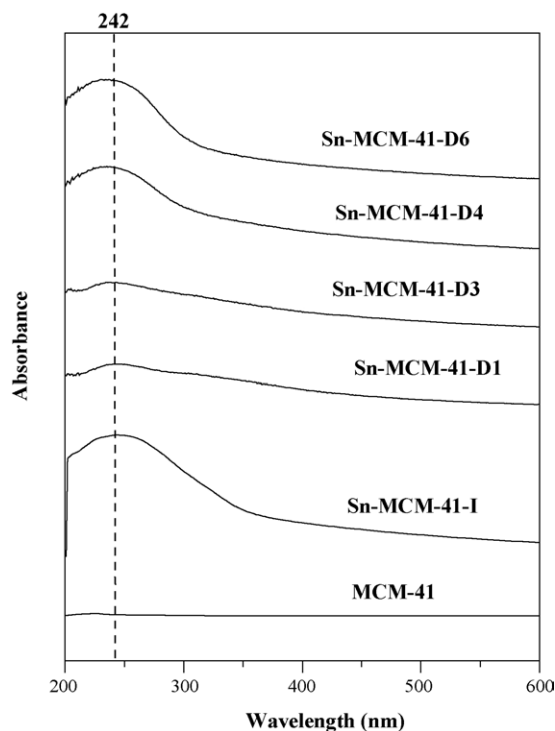


Fig. 6. Diffuse reflectance UV-vis spectra of MCM-41 catalysts.

species [18]. In addition, when Sn was incorporated on kenyaite by CVD an additional absorption band at  $291\text{ nm}$  was observed, indicating that Sn-Ken-C may also contain hexacoordinated polymeric Sn–O–Sn type species [13].

### 3.2. Catalytic activity

As can be observed in Table 3, when the  $\beta$ -pinene/paraformaldehyde ratio increased nopol yield decreased over Sn-Ken-A. Therefore, an excess of paraformaldehyde is required in order to obtain high  $\beta$ -pinene conversion and nopol selectivity. As the amount of Sn-Ken-A was reduced to a half,  $\beta$ -pinene conversion remained relatively constant and the selectivity to nopol decreased. Using aqueous formaldehyde, instead of paraformaldehyde, catalytic activity

Table 3

Activity of Sn-kenyaite catalysts in the Prins condensation of  $\beta$ -pinene

Catalyst	$\beta$ -Pinene/mmol paraformaldehyde	Conversion (%)	Selectivity (%)
Sn-Ken-A	0.5	44.2	98.5
Sn-Ken-A	0.5 <sup>a</sup>	45.7	78.0
Sn-Ken-A	0.5 <sup>b</sup>	7.2	90.1
Sn-Ken-A	1.0	41.7	78.8
Sn-Ken-A	2.0	25.3	97.7
Sn-Ken-B	0.5	50.8	98.1
Sn-Ken-C	0.5	46.3	94.4

Reaction conditions: 25 mg catalyst, 0.5 ml toluene, 0.25 mmol  $\beta$ -pinene,  $90^\circ\text{C}$ , 6.5 h.

<sup>a</sup> 13 mg catalyst.

<sup>b</sup> Aqueous formaldehyde instead of paraformaldehyde.

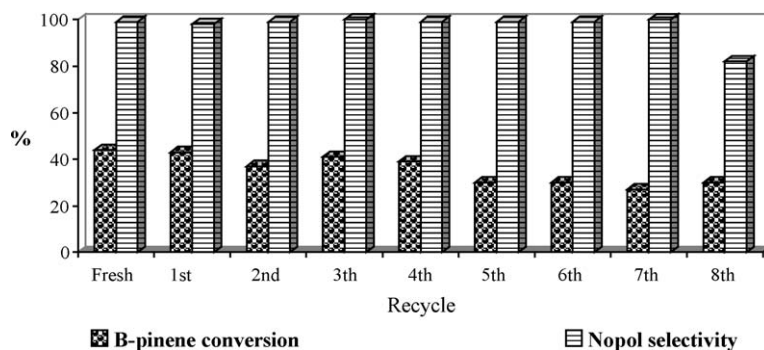


Fig. 7. Sn-Ken-A recycled. Reaction conditions: 25 mg catalyst, 0.5 ml toluene, 0.25 mmol  $\beta$ -pinene, 0.5 mmol paraformaldehyde, 90 °C, 6.5 h. Catalyst was recovered by filtration, washed at 50 °C with acetone and dried at 100 °C.

decreased, suggesting that the absence of water is required to obtain high nopol yields.

As observed in Table 3, Sn-kenyaite catalysts are selective (>94%) to nopol, particularly over catalysts synthesized by ion exchange. Besides, Sn loadings above 4.64 wt% do not have a significant effect on the catalytic activity of these catalysts. Under these conditions, diffusion

limitations are important, since reaction becomes faster as the Sn content increases. Over Sn-Ken-A catalyst,  $\beta$ -pinene conversion was approximately constant between the second and the fourth recycling; then, it decreased, showing a constant conversion between the fifth and eighth recycling (Fig. 7). Conversion of  $\beta$ -pinene over Sn-Ken-B decreased about 21% in the first reusing; then, it remained constant in

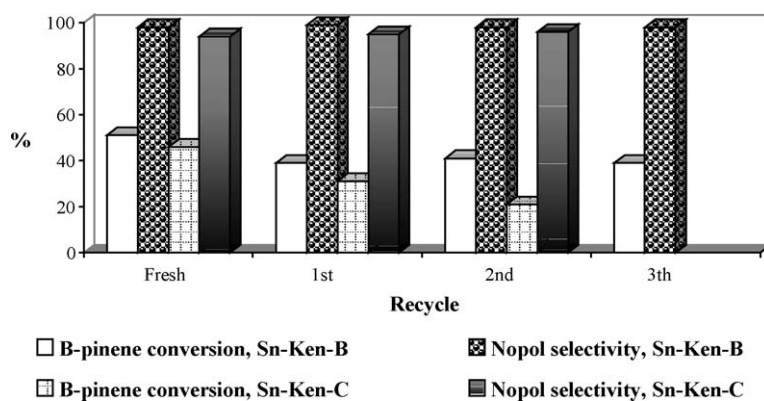


Fig. 8. Sn-Ken-B and Sn-Ken-C recycled. Reaction conditions: 25 mg catalyst, 0.5 ml toluene, 0.25 mmol  $\beta$ -pinene, 0.5 mmol paraformaldehyde, 90 °C, 6.5 h. Catalyst was recovered by filtration, washed at 50 °C with acetone and dried at 100 °C.

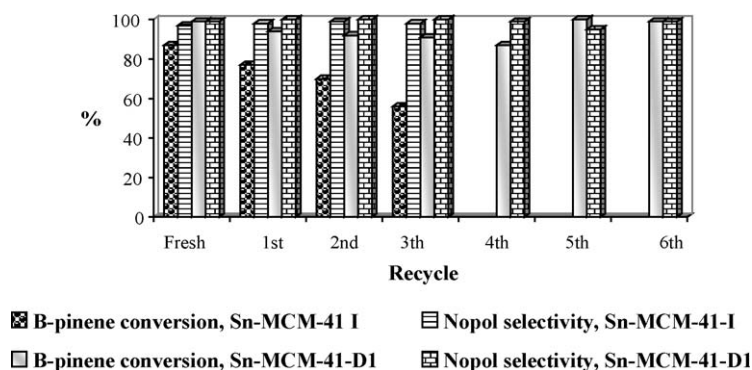


Fig. 9. Sn-MCM-41-I and Sn-MCM-41-D1 recycled. Reaction conditions: 50 mg catalyst, 1 ml toluene, 0.5 mmol  $\beta$ -pinene, 1 mmol paraformaldehyde, 90 °C, 1 h. The catalyst was recovered by filtration, washed at 50 °C with acetone and dried at 100 °C. Recovered catalyst from 4th recycle was also calcined at 550 °C before reusing it on the 5th recycle.

Table 4  
Activity of several Sn-MCM-41 catalysts on the Prins condensation of  $\beta$ -pinene

Catalyst	$\beta$ -Pinene conversion (%)	Nopol selectivity (%)
Sn-MCM-41-D1	99.3	98.7
Sn-MCM-41-D2	97.8	99.8
Sn-MCM-41-D3	96.7	98.1
Sn-MCM-41-D4	95.2	98.5
Sn-MCM-41-D5	96.7	97.8
Sn-MCM-41-D6	83.8	92.4
Sn-MCM-41-D7	78.5	96.2
Sn-MCM-41-I	87	97
MCM-41 <sup>a</sup>	10	100

Reaction conditions: 0.5 mmol of  $\beta$ -pinene, 1 mmol paraformaldehyde, 50 mg of catalyst, 1 ml of toluene, 90 °C, 1 h.

<sup>a</sup> 100 mg of catalyst.

the following two runs (Fig. 8). Sn-Ken-C deactivated faster. Conversion decreased to 55% after the second recycling (Fig. 8).

Sn-MCM-41 catalysts are much more active and selective to nopol (Table 4; Fig. 9). Table 4 lists conversion and selectivity of selected catalysts synthesized by chemical vapor deposition using different amounts of SnCl<sub>4</sub>. The results are compared with a catalyst sample synthesized by impregnation, Sn-MCM-41-I. Nopol selectivity obtained was higher than 91% with all Sn-MCM-41 catalysts tested. A Sn loading as low as 0.03 mmol Sn/g catalyst is enough for obtaining high nopol yield (98%). The conversion of  $\beta$ -pinene over MCM-41 is much lower than that obtained over MCM-41 doped with a small amount of Sn, but the selectivity to nopol is 100%. No Sn leaching was observed in catalysts containing less than 0.51 mmol Sn/g catalyst. The catalytic activity of Sn-MCM-41-D1 was maintained after six reactions (see Fig. 9). Higher Sn loadings led to catalyst leaching, i.e. Sn-MCM-41-D13. Sn leaching problems were also detected over Sn-MCM-41-I prepared by impregnation, (see Fig. 9). In the third run,  $\beta$ -pinene conversion dropped to 56%.

#### 4. Conclusions

The CVD method used in this work allows a controlled Sn modification of MCM-41. The lowest Sn loadings tested gave the highest nopol yields suggesting that highly dispersed Sn species promote nopol production over MCM-41.

High nopol selectivities were obtained over Sn-kenyaite catalysts but  $\beta$ -pinene conversion varied around 50%. Ion exchange showed to be a more effective method than CVD to obtain active Sn-Ken materials for the Prins condensation of  $\beta$ -pinene. However, a diminished catalytic activity and surface area were observed after reaction.

MCM-41 showed to be a more suitable Sn support than kenyaite for the Prins condensation of  $\beta$ -pinene to obtain nopol, because higher catalytic activity was observed over Sn-MCM-41 catalysts even with lower Sn loadings than those in Sn-kenyaite materials.

#### Acknowledgement

The authors gratefully acknowledge COLCIENCIAS-BID and Universidad de Antioquia for sponsoring this work through the Project 1115-05-040-99.

#### References

- [1] K. Bauer, D. Garbe, H. Surburg (Eds.), Common Fragrance and Flavor Materials. Preparation Properties and Uses, VCH Verlagsgesellschaft, 1990, p. 59.
- [2] J.P. Bain, J. Am. Chem. Soc. 68 (1946) 638.
- [3] A.L. Villa de P, E. Alarcón, C. Montes de C, Chem. Commun. (2002) 2654.
- [4] J.S. Beck, J.C. Vartuli, G.J. Kennedy, C.T. Kresge, W.J. Roth, S.E. Schramm, Chem. Mater. 6 (1994) 1816.
- [5] U.R. Pillai, E. Sahle-Demessie, Chem. Commun. (2004) 826.
- [6] K. Kosuge, A. Yamazaki, A. Tsunashima, R. Otsuka, J. Ceram. Soc. Jpn., Int. Ed. 100 (1992) 338.
- [7] G.G. Almond, R.K. Harris, K.R. Franklin, J. Mater. Chem. 7 (1997) 681.
- [8] O.-Y. Kwon, S.-Y. Jeong, J.-K. Suh, J.-M. Lee, Bull. Korean Chem. Soc. 16 (1995) 737.
- [9] H.P. Eugster, Science 157 (1967) 1177.
- [10] M. Grün, K.K. Unger, A. Matsumoto, K. Tsumumi, Micropor. Mesopor. Mater. 27 (1999) 207.
- [11] J.S. Dailey, T.J. Pinnavaia, Chem. Mater. 4 (1992) 855.
- [12] C.-M. Leu, Z.-W. Wu, K.-H. Wei, Chem. Mater. 14 (2002) 3016.
- [13] K. Chaudhari, T.K. Das, P.R. Rajmohan, K. Lazar, S. Sivasanker, A.J. Chandwadkar, J. Catal. 183 (1999) 281.
- [14] Y. Huang, Z. Jiang, W. Shwieger, Chem. Mater. 11 (1999) 1210.
- [15] P. Fejes, J.B. Nagy, K. Kovács, G. Vankó, Appl. Catal., A 145 (1996) 155.
- [16] B. Jezowska-Trzebiatowska, J. Hanuza, W. Wojciechowski, Spectrochim. Acta 23A (1967) 2631.
- [17] T.Kr. Das, K. Chaudhari, A.J. Chandwadkar, S. Sivasanker, J. Chem. Soc., Chem. Commun. (1995) 2495.
- [18] N.K. Mal, A.V. Ramaswamy, J. Mol. Catal. 105 (1996) 149.